



Modeling Plasma Interactions with Space-Borne Instrumentation



J. H. Klenzing, G. D. Earle, R. A. Heelis

William B. Hanson Center for Space Sciences, The University of Texas at Dallas

Introduction

We have developed a simulation of ion interaction with the biased grids of a Retarding Potential Analyzer (RPA), which is one of the fundamental instruments of space science. The analysis technique used in the RPA is also essential to the measurements made by the Ram Wind Sensor, a neutral wind anemometer scheduled to be launched as part of C/NOFS in 2008. Both instruments measure the distribution of particle flux as a function of ion energy by using biased grids as an energy filter for collected particles. The goal of this research is use simulations of this interaction to create a more accurate data analysis technique.

The RPA as an Energy Filter

Figure 1 shows a sample ion population and the corresponding IV curve collected by an idealized RPA. The RPA functions by successively retarding ions below a specific energy. This allows us to relate a collected current-voltage (IV) curve to a density distribution.

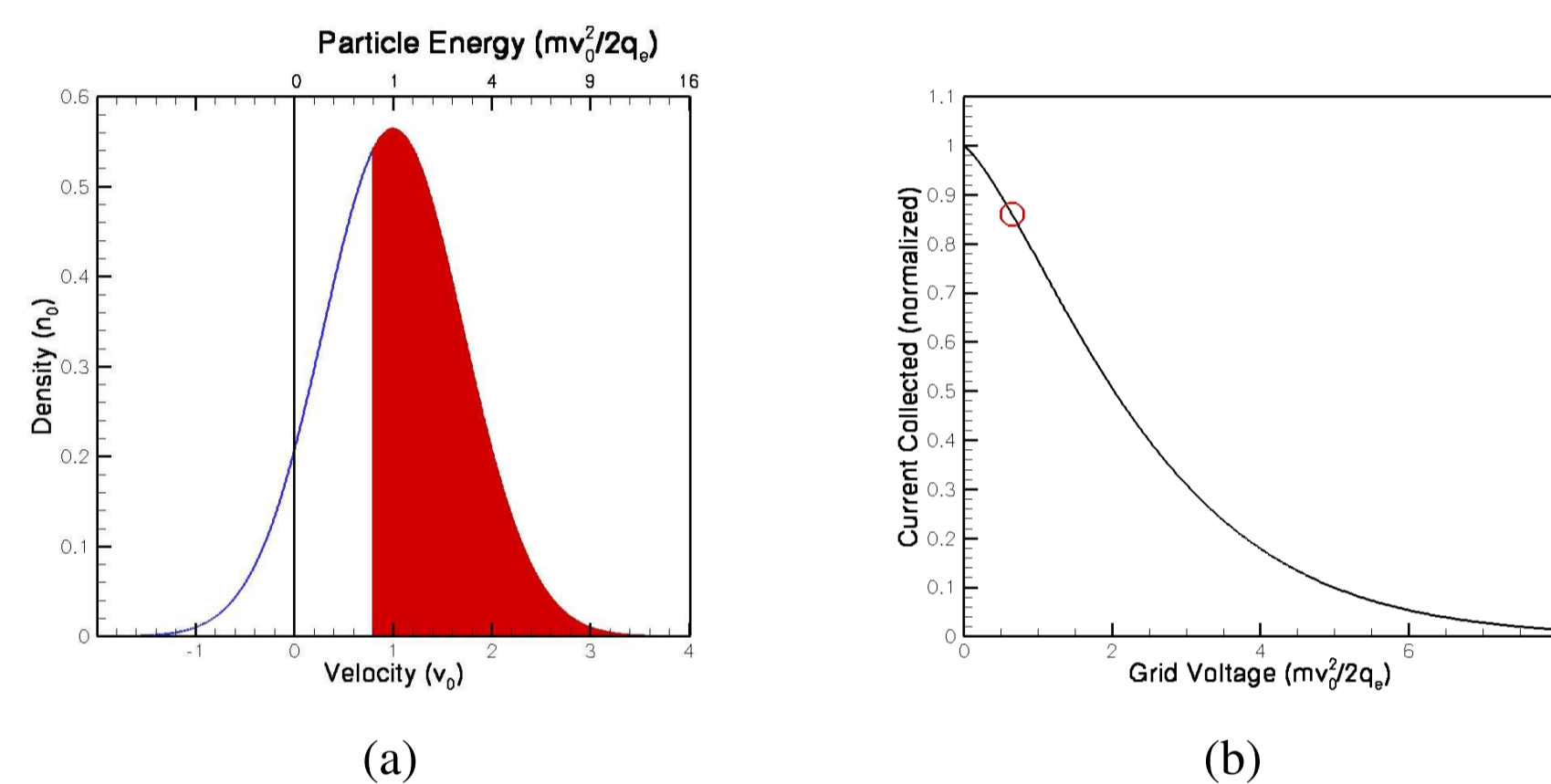


Figure 1: A sample density distribution and the corresponding IV curve. The thermal velocity has been artificially inflated for purposes of illustration. The shaded portion of (a) illustrates the ions collected for a particular bias voltage. Ions with a negative velocity relative to the collector are moving away from the collector and cannot be collected. The circle on the curve in (b) indicates the current collected for the applied IV in (a).

We can describe the current through some collector area A of a standard RPA (which is laid perpendicularly to the z -axis and is at rest with respect to the ions) with the following equation

$$I(\phi_r) = qA \int_{v_x, v_y} \int_{v_z=0}^{\infty} \chi(\phi_r, \vec{v}) v_z \mathcal{D}(\vec{v}) d\vec{v} \quad (1)$$

where $\mathcal{D}(\vec{v})$ is the density distribution of the ion population. The function $\chi(\vec{v}, \phi_r)$ describes the transmission of particles through the energy filter for a given applied bias (ϕ_r), as only a specific subset of energies will contribute to the collected current. Note that we integrate over all bounds in the plane of the collector, while we exclude those particles moving in the $-z$ direction (away from the collector). In the idealized case from Knudsen [1966], we consider the incoming ion distribution as a drifting Maxwellian. Because this function is symmetric over v_x and v_y , we can collapse this volumetric integral to a line integral along v_z . The idealization sets the transmission function as a step function, where all ions below the stopping value are rejected and a constant fraction of ions above the stopping value is transmitted. This fraction is equal to the optical transparency of the grid structure (χ_a), or those particles unblocked by the grid. Equation 1 reduces to the form used by Whipple [1959], which integrates to the simple analytic form

$$I = \frac{qA\chi_a n_0 v_{z0}}{2} \left[1 + \text{erf}(\kappa) + \frac{v_{th}}{v_{z0}\sqrt{\pi}} e^{-\kappa^2} \right] \quad (2)$$

where $\kappa = (v_{z0} - \sqrt{2q\phi_r/m})/v_{th}$, and ϕ_s is the stopping potential. This is the standard equation currently used to analyze RPA data.

Problems with the Ideal Assumptions

The assumptions used to derive Equation 2 do not hold for real grids because the potential in the plane of the grid is non-uniform, allowing ions with energies less than the stopping energy ($\mathcal{E}_s = q\phi_r$) to leak through the filter [Hanson 1972], as seen in Figure 2b. The level of leakage will be determined by the specific instrument geometry and the potentials applied throughout. For example, ions having energies slightly greater than \mathcal{E}_s will be lensed around the grid wire. This will increase the transmission for these particular energies to a value greater than the optical transparency. Both of these effects will increase the total current collected for a given applied bias. For real grid structures, it is difficult to calculate an analytic expression for $\chi(\vec{v})$ without making great sacrifices in the accuracy of the model. To look at a less-idealized model similar to a real RPA, we calculate discrete values of transmission using numerical analysis for a given set of inputs.

ANSYS Simulation

We can use ANSYS (a multiphysics simulation package) to calculate the electric fields everywhere within a sample model of the RPA, as shown in Figure 2a. Ions can be placed in the field-free region in the front of the model with a specified charge, mass, and initial velocity vector. To calculate χ , a large number of ions can be placed in the front of the model for a given ram energy (\mathcal{E}_\perp or $\frac{1}{2}mv_z^2$), angle of attack (α), and azimuthal angle (β). The transmission ratio is needed for each applied potential (ϕ_r). The number of ions (3000) was determined by the level of variation found in the simulation. The ions are placed in the xy -plane with randomly generated coordinates over a repeating area. The transmission ratio is calculated as the fraction of ions which pass the energy filter and are unblocked by the grid wires for a given set of input parameters.

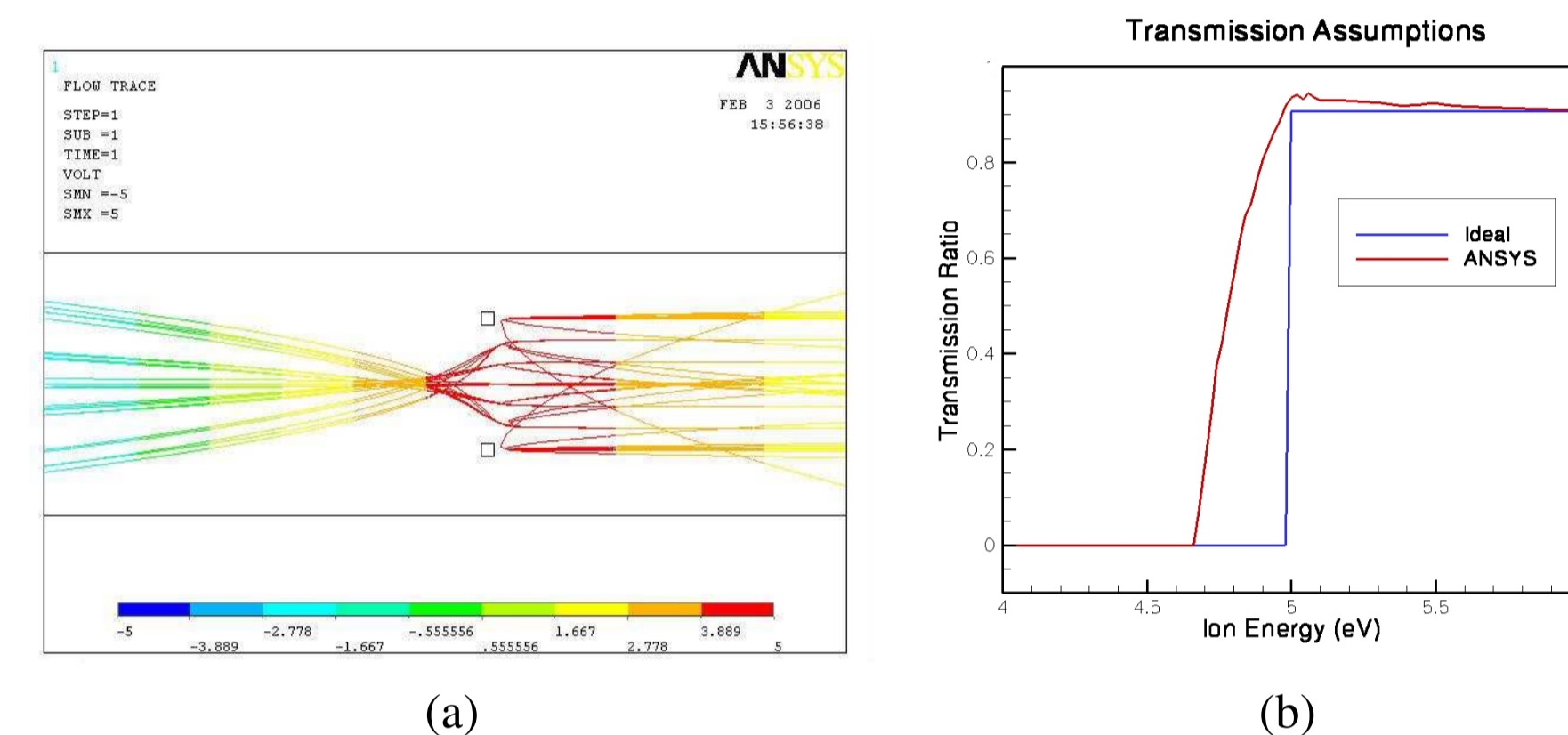


Figure 2: The transmission functions are generated through ANSYS by calculating individual ion tracks (a). The transmission is taken to be the ratio of ions which pass through the retarding grid to the total ions. Those which are deflected, reflected, or collected by the grids are neglected. The transmission values for $\phi_r = 5V$ are compared to the idealized transmission ratios in (b). Note that transmission is always greater than expected, yielding larger fluxes for all incoming ion energies.

IV Simulation

Once the full set of $\chi(\phi_r, \mathcal{E}_\perp, \alpha, \beta)$ has been generated, an IV curve representative of a given three-dimensional ion velocity distribution may be generated by the use of Monte Carlo simulation. This is done by numerically integrating Equation 1 by the sample-mean method [Rubinstein 1981]. The integral is defined as

$$I(\phi_r) = \frac{V_V}{N} \sum_{a=1}^N \chi_a(\phi_r) v_{za} \mathcal{D}(\vec{v}_a) \quad (3)$$

where V_V is the volume of the velocity space, N is the number of points generated, and $\chi_a(\phi_r)$ is the $\chi(\phi_r, \mathcal{E}_\perp, \alpha, \beta)$ associated with the set of \vec{v}_a produced by the random number generator. The three variables were generated using the ran2.f routine from Press [1992]. The simulation is run for 10^7 points in the 3D space, and the distribution function is taken to be a drifting Maxwellian of O^+ centered about \vec{v}_0 and with thermal velocity $v_{th} = \sqrt{2kT/m}$. A set of 1000 IV curves was generated for random input parameters of \vec{v}_0 and T . Since the resultant IV curves were normalized, variation of the density parameter (n_0) was not studied. A companion set of curves was generated using the analytic expression (Equation 2) for the same set of input parameters. The input values for these parameters are shown in Figure 3a. The angle of attack was varied by adding random levels of two-dimensional cross-track drift, which is not accounted for in current fitting techniques. Figure 3b shows a sample set of simulated RPA data using both the analytic technique and the Monte Carlo simulation.

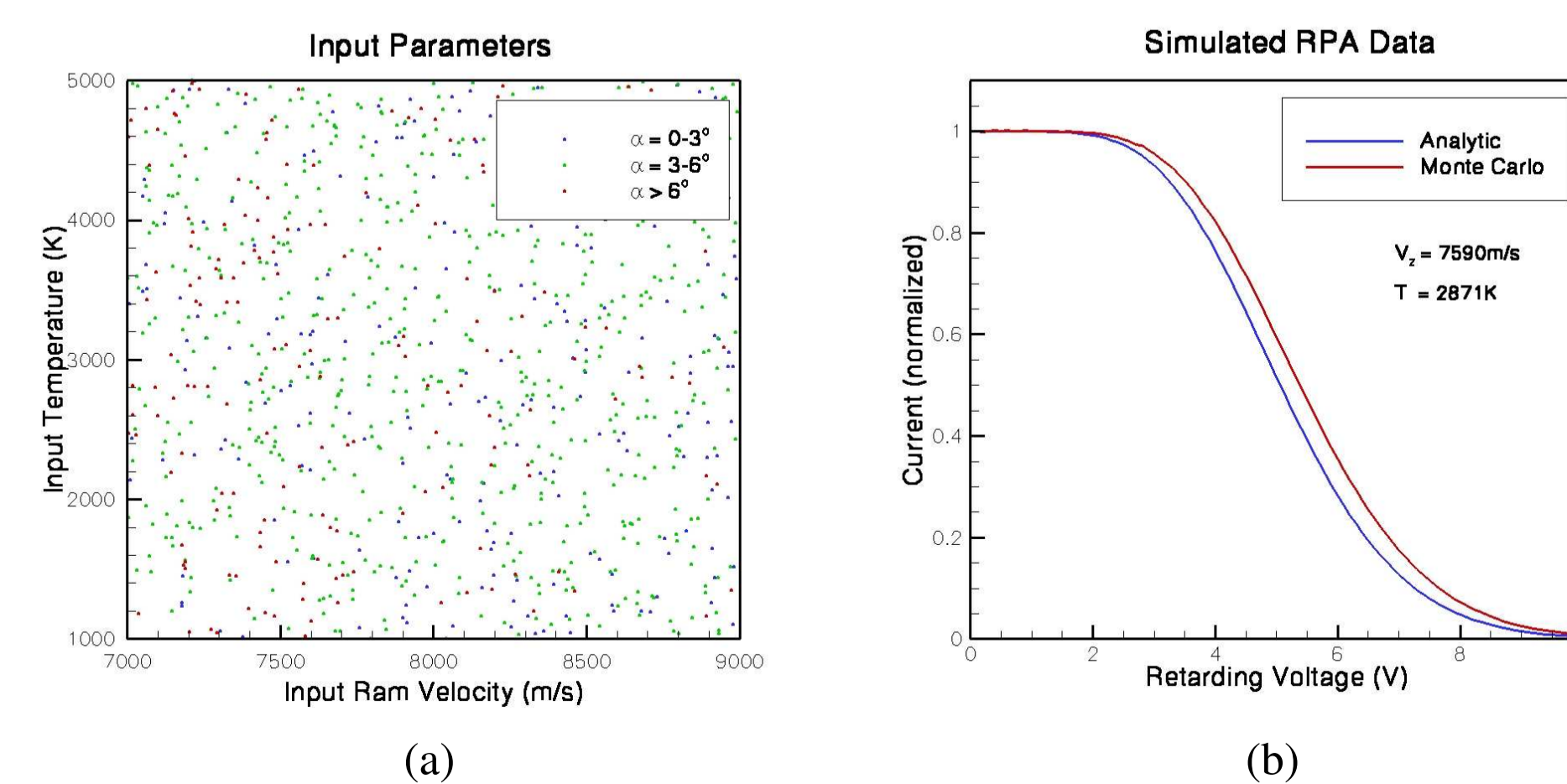


Figure 3: (a) is the set of randomly generated input parameters used to generate the simulated IV curves for this study. (b) is a sample pair of IV curves for a single set of input parameters. The sample curves were generated using both the analytic (Equation 2) and Monte Carlo (Equation 3) techniques. Simulated data like those shown in (b) were generated for all input parameters shown in (a).

Inherent Deviations in Inferred Parameters

All of these curves were fit using the Levenberg-Marquardt non-linear fitting routine [Press 1992] optimized to find the best ram velocity (v_z) and ion temperature (T). This is the same routine currently used to analyze RPA data from DMSP. Note that it force fits the data to the analytic expression (Equation 2), which will yield inherent deviations in the fit parameters because of the idealized assumptions used in deriving Equation 2. The fit results are shown in Figure 4. We found that there is a consistent positive offset in the fitted ram velocities (a), and a small deviation in the fitted ion temperatures (b).

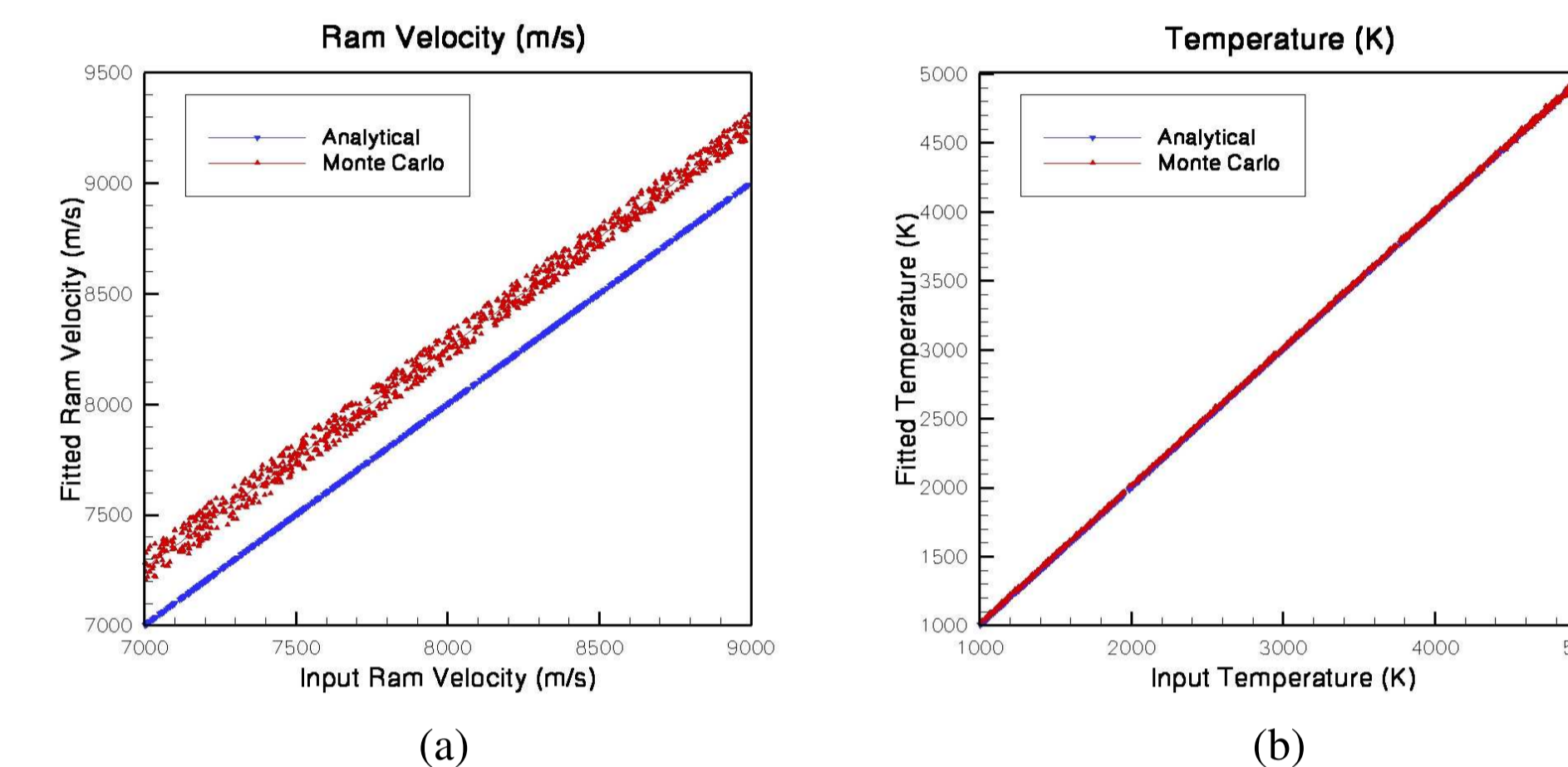


Figure 4: The fit values given by the Levenberg-Marquardt non-linear fit routine for both ion ram velocity (a) and ion temperature (b). The fits were done for IV curves generated both by the analytic equation and the ANSYS/Monte Carlo technique, as shown in Figure 3b. Note the consistent positive offset in the fitted ram velocities.

Figures 5 and 6 show the deviations between the two fits (defined as the fit parameter from the Monte Carlo curves minus the fit parameter from the analytic curves) as a function of several input parameters of interest.

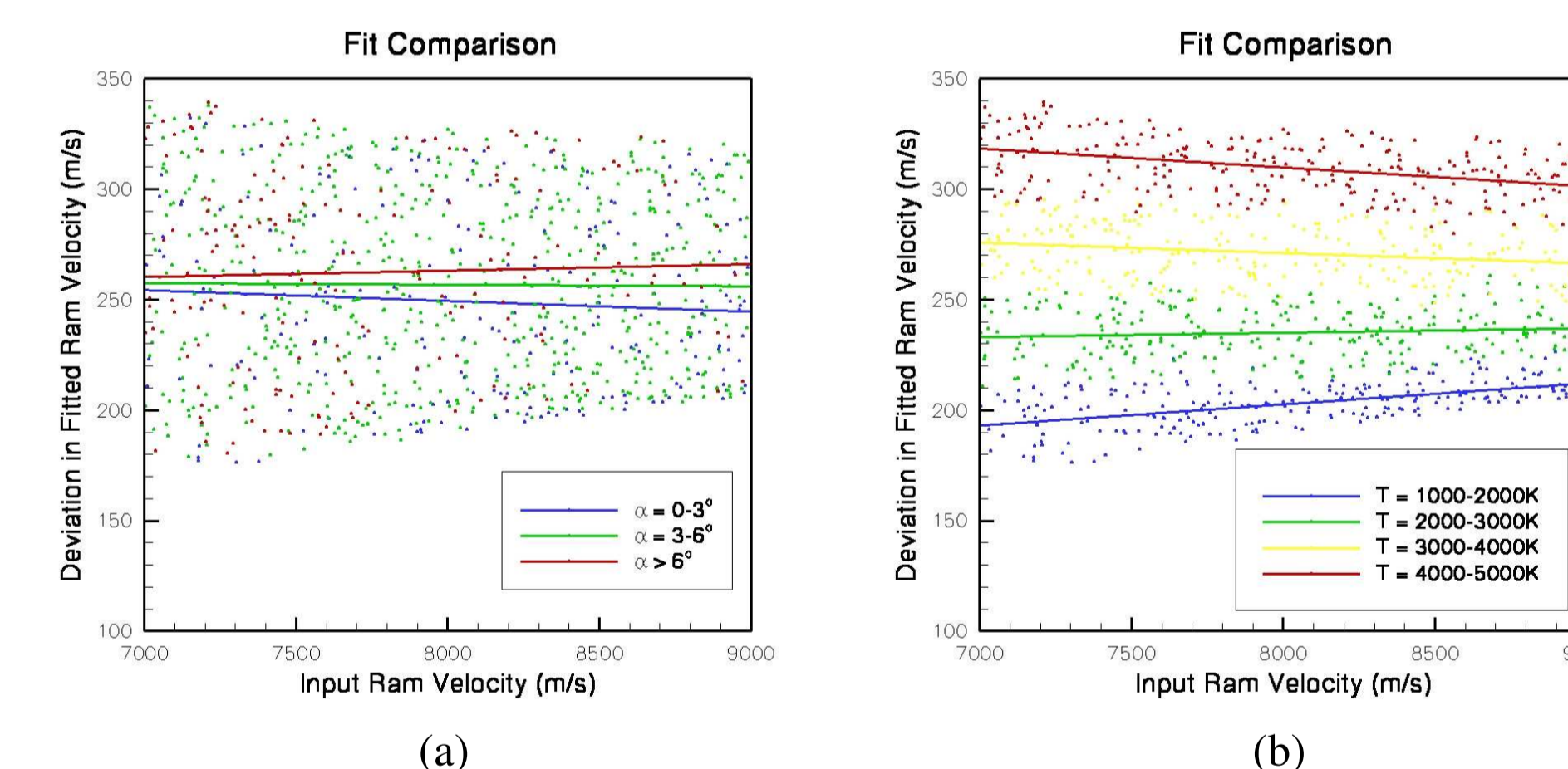


Figure 5: The deviation in fitted ram velocity values due to the effects of a non-ideal grid as a function of input values for 1000 simulated data sets, along with linear fits. (a) is grouped by input angle of attack. (b) is grouped by input temperature. The fits show a consistent positive deviation in ram velocity when the ideal assumptions are used in the fitting technique.

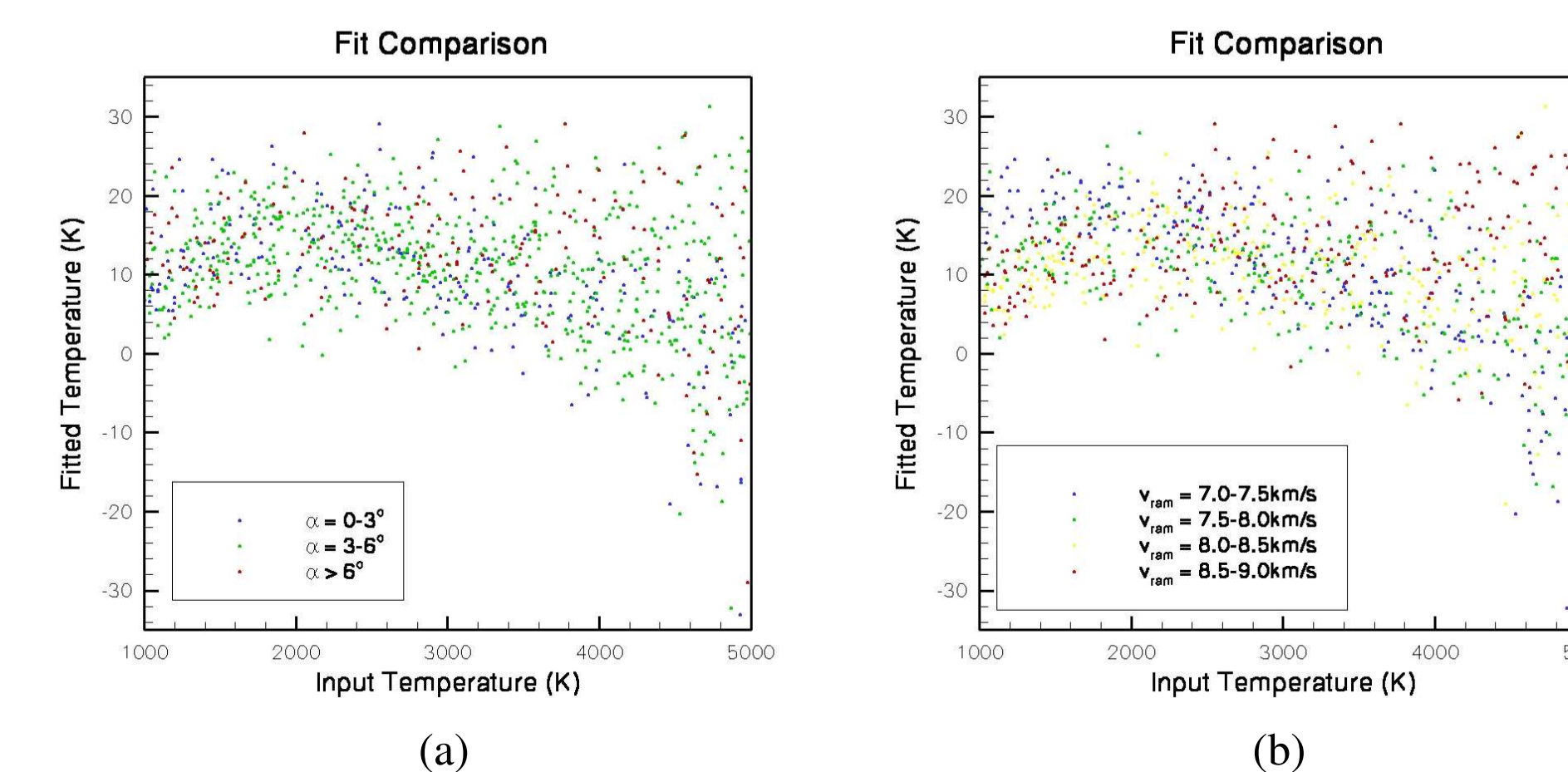


Figure 6: The deviation in fitted temperature values due to the effects of a non-ideal grid as a function of input values for 1000 simulated data sets. (a) is grouped by input angle of attack. (b) is grouped by input ram velocity. The scatter shows the inherent uncertainty in the temperature fits due to non-ideal grid effects.

Discussion

The fits in Figure 5 show a consistent offset in the inferred ram velocity on the order of $175 - 340$ m/s. The lower end of this spectrum is comparable to the results found by Chao [2003]. Note that there is a small correlation to angle of attack in the fit parameters (Figure 5a), whereas the idealized form assumes that there is no variation if a cross-track drift is added to the data. There is a marked variation of fitted velocity as a function of temperature, as illustrated in Figure 5b.

The fits show a consistent overestimate of temperature for those values below $4000K$, with possible underestimates for input temperatures above this as shown in Figure 6. The total range of fit deviations is $\pm 30K$. The inherent uncertainty (scatter) in the inferred temperature increases significantly for higher input temperatures.

The results suggest that there is a systematic overestimate of ram velocity values and an inherent uncertainty in temperature values as currently analyzed by a single-grid RPA. This effect can be extrapolated to apply to a double-grid RPA, such as that flown on DMSP, though the effect may be less pronounced.

New analysis procedures based on results such as these can be applied to both RPA instruments and to the newly developed Ram Wind Sensor for C/NOFS.

Conclusions

- The simulation results confirm the work of Chao [2003] for deviations in ram velocity, showing substantial deviations on the order of $175 - 340$ m/s which increase as ion temperature increases.
- Deviations in ion ram velocity increase if a cross-track ion drift is present.
- Deviations in inferred temperatures have a large spread, ranging from $\pm 30K$.
- Results indicate that a computational analysis technique to infer physical parameters from RPA data may significantly improve the quality of geophysical data.

Future Work

There are many parameters to still be studied using this technique, including simulated processing of data as typically seen in space, fits for multiple species, etc. The complete results of this study will be published later this year. Complicated geometries such as the double-grid energy filter promise more interesting results.

References

- Chao, C.K., S.-Y. Su, H.C. Yeh, Grid effects on the derived ion temperature and ram velocity from the simulated results of the retarding potential analyzer data, *Adv. Space Res.*, **32**, 2361, 2003
- Hanson, W.B., D.R. Frame, J.E. Midgely, Errors in retarding potential analyzers caused by nonuniformity of the grid-plane potential, *J. Geophys. Res.*, **77**, 1914-1922, 1972
- Knudsen, W.C., Evaluation and demonstration of the use of retarding potential analyzers for measuring several ionospheric quantities, *J. Geophys. Res.*, **71**, 4669-4678, 1966
- Press, W. H., S. A. Teukolsky, W. T. Vetterling, Brain P. Flannery, Numerical Recipes in FORTRAN 77, Second Edition, Cambridge University Press, 1992
- Rubinstein, R. Y., Simulation and the Monte Carlo Method, John Wiley and Sons, 1981
- Whipple, E.C., The Ion Trap Results in Exploration of the Upper Atmosphere with the Help of the Third Soviet Sputnik, *Proc. of the Inst. of Rad. Eng.*, **47**, (11), 2023-2024, 1959

Acknowledgments

This work was supported by NASA grant NNG05-GL70H. The authors would like to thank Dr. Robin Coley for assistance with the curve-fitting procedure and Dr. Robert Pfaff for sponsoring this project for NASA.

For More Information

Please contact jeffk@utdallas.edu. This poster is available online at www.utdallas.edu/~jeffk/CEDAR/poster07.pdf